

GRB010222: afterglow emission from a rapidly decelerating shock ^{*}

N. Masetti¹, E. Palazzi¹, E. Pian^{2,1}, F. Mannucci³, L.A. Antonelli⁴, A. Di Paola⁴, P. Saracco⁵, S. Savaglio⁴, L. Amati¹, C. Bartolini⁶, S. Bernabei^{7,8}, D. Bettoni⁹, S. Covino⁵, S. Cristiani¹⁰, S. Desidera¹¹, S. Di Serego Alighieri¹², R. Falomo⁹, F. Frontera^{1,13}, F. Ghinassi¹⁴, A. Guarnieri⁶, A. Magazzù¹⁴, R. Maiolino¹², M. Mignoli⁷, L. Nicastro¹⁶, M. Pedani¹⁴, A. Piccioni⁶, B.M. Poggianti⁹, V. Testa⁴, G. Valentini¹⁵, and A. Zacchei¹⁴

¹ Istituto Tecnologie e Studio delle Radiazioni Extraterrestri, CNR, Via Gobetti 101, I-40129 Bologna, Italy

² Osservatorio Astronomico di Trieste, Via G.B. Tiepolo 11, I-34131 Trieste, Italy

³ Centro per l'Astronomia Infrarossa e lo Studio del Mezzo Interstellare, CNR, Largo E. Fermi 5, I-50125 Florence, Italy

⁴ Osservatorio Astronomico di Roma, via di Frascati 33, I-00040 Monteporzio Catone, Italy

⁵ Osservatorio Astronomico di Brera, via Bianchi 46, I-23807 Merate, Italy

⁶ Dipartimento di Astronomia, Università di Bologna, Via Ranzani 1, I-40127 Bologna, Italy

⁷ Osservatorio Astronomico di Bologna, Via Ranzani 1, I-40127 Bologna, Italy

⁸ Instituto de Astrofísica de Canarias, C/ Vía Láctea s/n, E-38200, La Laguna, Tenerife, Spain

⁹ Osservatorio Astronomico di Padova, Vicolo dell'Osservatorio 5, I-35122 Padua, Italy

¹⁰ Dipartimento di Astronomia, Università di Padova, Vicolo dell'Osservatorio 5, I-35122 Padua, Italy

¹¹ Osservatorio Astronomico di Asiago, Via dell'Osservatorio 8, I-36012, Asiago, Italy

¹² Osservatorio Astrofisico di Arcetri, Largo E. Fermi 5, I-50125 Florence, Italy

¹³ Dipartimento di Fisica, Università di Ferrara, via Paradiso 12, I-44100 Ferrara, Italy

¹⁴ Telescopio Nazionale Galileo, Roque de Los Muchachos Astronomical Observatory, P.O. Box 565, E-38700 Santa Cruz de La Palma, Spain

¹⁵ Osservatorio Astronomico di Collurania-Teramo, Via Maggini, I-64100 Teramo, Italy

¹⁶ Istituto di Fisica Cosmica ed Applicazioni all'Informatica, CNR, via ugo La Malfa 153, I-90146 Palermo, Italy

Received March 19, 2001; Accepted May 23, 2001

Abstract. The GRB010222 optical and near-infrared (NIR) afterglow was monitored at the TNG and other Italian telescopes starting ~ 1 day after the high-energy prompt event. The BVR light curves, which are the best sampled, are continuously steepening and can be described by two power laws, $f(t) \propto t^{-\alpha}$, of indices $\alpha_1 \sim 0.7$ and $\alpha_2 \sim 1.3$ before and after a break occurring at about 0.5 days after the GRB start time, respectively. This model accounts well also for the flux in the U , I and J bands, which are less well monitored. The temporal break appears to be achromatic. The two K -band points are not consistent with the above behaviour, and rather suggest a constant trend. A low-resolution optical spectrum has also been taken with TNG. In the optical spectrum we found three absorption systems at different redshifts (0.927, 1.155 and 1.475), the highest of which represents a lower limit to, and probably coincides with, the redshift of the GRB. The broad-band optical spectral energy distributions do not appear to vary with time, consistently with the achromatic behaviour of the light curves. We compare our measurements with different afterglow evolution scenarios and we find that they favor a transition from relativistic to non-relativistic conditions in the shock propagation.

Key words. Gamma rays: bursts — Radiation mechanisms: non-thermal — Line: identification — Cosmology: observations

1. Introduction

The light curves of Optical Transients (OTs) associated with GRBs are generally described by single power laws $f(t) \propto t^{-\alpha}$ with indices $\alpha \simeq 1.1 - 2$. However, in a number of well monitored cases a change in the light decay rate at about 0.5-1 days after the GRB was detected with a transition to a steeper power law behaviour. The power law indices before and after the temporal break are typically in the range 0.7-1 and 1.7-2.4, respectively (GRB990123: Fruchter et al. 1999, Castro-Tirado

Send offprint requests to: Nicola Masetti, masetti@tesre.bo.cnr.it

* Based on observations collected at: the Italian Telescopio Nazionale Galileo (TNG), operated on the island of La Palma by the Centro Galileo Galilei of the CNAO (Consorzio Nazionale per l'Astronomia e l'Astrofisica) at the Spanish Observatorio del Roque de los Muchachos of the Instituto de Astrofísica de Canarias; the Asiago Astronomical Observatory, Italy; the Bologna Astronomical Observatory in Loiano, Italy; the Campo Imperatore Astronomical Observatory, Italy, and; TIRGO infrared observatory, Switzerland

et al. 1999, Kulkarni et al. 1999; GRB990510: Stanek et al. 1999, Harrison et al. 1999, Israel et al. 1999; GRB990705: Masetti et al. 2000a; GRB000926: Fynbo et al. 2001a). This behaviour can be caused by the deceleration of a relativistic jet in a homogeneous medium (Sari et al. 1999, Rhoads 1999), or by expansion in a wind (Chevalier & Li 1999, 2000), or by the transition between relativistic and Newtonian conditions in the plasma expansion (Dai & Lu 1999). Fits to multiwavelength data of individual afterglows with the above models have been proved to be satisfactory (Dai & Lu 1999, Panaitescu & Kumar 2000). The multiwavelength optical and near-infrared (NIR) spectra of OTs are generally well accounted for by synchrotron radiation in a relativistically expanding shock, and are described by power laws of different characteristic indices, depending on the location of injection and cooling breaks, and temporal evolution thereof (Sari et al. 1998). Both the fading rate and the spectral slopes are determined by the shape of the electron distribution, in different ways, according to the geometry of the emitting region. Departures of the optical-NIR spectral slopes from those expected based on the flux temporal decrease are often interpreted as due to absorption of the OT light within the GRB host galaxy (e.g. Palazzi et al. 1998, Dal Fiume et al. 2000, Klose et al. 2000, Price et al. 2001a).

GRB010222 was simultaneously detected by the Gamma-Ray Burst Monitor (GRBM) and the Wide Field Camera (WFC) unit 1 onboard *BeppoSAX* on 2001 Feb 22.30799 UT (Piro 2001a,b) as one of the most intense GRBs observed by both the GRBM and WFC. A quick repointing of the satellite allowed the detection of the X-ray afterglow at a position consistent with that of the prompt event (Gandolfi 2001). A detailed analysis of the high-energy data is presented by Zand et al. (2001).

Many observers started a ground-based campaign in order to search for the GRB afterglow at lower wavelengths. A bright transient source ($R \sim 18.4$) was independently detected in the optical by Henden (2001a,b; see also Henden & Vrba 2001) and McDowell et al. (2001) about 4 hours after the GRB. The object, which is not present in the DSS-II sky survey, is at coordinates (J2000) $\alpha = 14^{\text{h}} 52^{\text{m}} 12^{\text{s}}.55$, $\delta = +43^{\circ} 01' 06''.2$ with an error of $0''.2$ along both directions (Henden & Vrba 2001), well inside the error box of both high-energy prompt event and X-ray afterglow as detected by the *BeppoSAX* Narrow Field Instruments. The OT is among the brightest ever observed associated with GRBs.

The fading behaviour of the object, first reported by Henden & Vrba (2001) and later confirmed by Stanek et al. (2001a,b), left little doubt on its afterglow nature. Assuming for the R -band flux a power law decay, typical of optical afterglows, Price et al. (2001b) and Fynbo et al. (2001a) measured a temporal slope $\alpha = 0.89 \pm 0.09$ and $\alpha = 0.86 \pm 0.01$, respectively. Masetti et al. (2001) reported that a steepening of the decay slope to $\alpha \sim 1.3$ occurred at about 1 day after the GRB start time.

Garnavich et al. (2001) acquired an optical spectrum of the OT soon after its detection. From the presence of Fe II and Mg II absorption features, they measured a redshift $z = 1.477$ for the afterglow. Jha et al. (2001a,b) also noticed the presence in the same spectrum of a second absorption system, located

at $z = 1.157$. A third absorption system at $z = 0.928$ in the optical spectrum of the afterglow was reported by Bloom et al. (2001). The farthest of the three systems appeared to be formed by substructures at slightly different redshifts, consistent with internal gas motions in galaxies (Castro et al. 2001).

A bright counterpart was also detected at NIR (Di Paola et al. 2001), submillimetric (Fich et al. 2001) and radio (Berger & Frail 2001) wavelengths.

The good sampling and the optical brightness of the GRB010222 afterglow have allowed a detailed study of its evolution at least up to about 40 days after the explosion. In this paper we present the results of the optical and NIR monitoring of the optical/NIR transient associated with GRB010222 conducted at various Italian telescopes and started about 1 day after the GRB. Section 2 illustrates the observations and the analysis of the photometric and spectroscopic data; the results are presented in Section 3 and discussed in Section 4.

2. Observations and data reduction

We observed the GRB010222 field at the 3.58-meter *Telescopio Nazionale Galileo* (TNG) in the Canary Islands (Spain), at the 1.8-meter ‘‘Copernicus’’ telescope at Cima Ekar of the ‘‘Leonida Rosino’’ Astronomical Observatory of Asiago (Italy), and at the University of Bologna 1.52-meter ‘‘G.D. Cassini’’ telescope in Loiano (Italy).

TNG was equipped with the spectrophotometer DOLoReS and a 2048×2048 pixels Loral CCD which allows covering a $9'.5 \times 9'.5$ field in imaging mode with a scale of $0''.275/\text{pix}$; the ‘‘Copernicus’’ telescope was carrying the AFOSC instrument whose 1100×1100 pixels SITE CCD has a field of view of $8'.5 \times 8'.5$ with a scale of $0''.47/\text{pix}$; the ‘‘Cassini’’ telescope was mounting the spectrophotometer BFOSC with a 1340×1340 pixels EEV CCD, a field of view of $12'.5 \times 12'.5$ and a scale of $0''.58/\text{pix}$.

NIR imaging in J and K bands was acquired at the AZT-24 1.1-meter telescope at Campo Imperatore (Italy) with SWIRCAM, a 256×256 pixels infrared camera with a field of view of $4'.4 \times 4'.4$ and a pixel scale of $1''.03/\text{pix}$, and in J and K_s at the 1.5-meter Gornergrat infrared telescope TIRGO (Switzerland) using the 256×256 pixels infrared camera ARNICA which has a $4' \times 4'$ field of view and a pixel scale of $0''.97/\text{pix}$. The K_s filter is centered at $2.12 \mu\text{m}$ and has a full width at half maximum of $0.34 \mu\text{m}$. For each NIR observation the total integration time was split into images of 30 s each, and the telescope was dithered in between.

The complete log of our imaging observations is reported in Table 1.

Two 30-min spectra, nominally covering the 3000-8000 Å optical range, were also acquired with TNG+DOLoReS between Feb 23.227 and Feb 23.274 UT. The use of DOLoReS Grism #1 secured a dispersion of $2.4 \text{ \AA}/\text{pix}$. The slit width was $1''.5$.

Optical images were debiased and flat-fielded with the standard cleaning procedure. In some cases, frames taken on the same night in the same band were summed together in order to increase the signal-to-noise ratio. In Fig. 1 we report our

Table 1. Journal of the optical and NIR observations of the GRB010222 afterglow. Magnitude uncertainties are at 1σ confidence level

Exposure start (UT)	Telescope	Filter	Total exposure time (s)	Seeing (arcsec)	Magnitude ¹
2001 Feb 22.982	AZT-24	<i>J</i>	2700	4.0	18.6±0.2 ²
23.056	Asiago	<i>R</i>	1200	3.8	19.75±0.05
23.063	Asiago	<i>R</i>	600	3.8	19.79±0.04
23.069	Asiago	<i>I</i>	600	3.8	19.27±0.06
23.082	AZT-24	<i>K</i>	2400	4.0	17.2±0.3 ²
23.083	Asiago	<i>I</i>	600	3.8	19.32±0.06
23.173	Loiano	<i>B</i>	2400	4.5	20.72±0.08 ³
23.199	Loiano	<i>V</i>	1800	4.0	20.37±0.10 ³
23.204	AZT-24	<i>J</i>	900	4.0	18.4±0.3 ²
23.211	TNG	<i>R</i>	120	1.1	20.00±0.01
23.219	TNG	<i>R</i>	120	1.1	20.01±0.01
23.280	TNG	<i>U</i>	300	1.1	20.34±0.03
23.284	TNG	<i>U</i>	300	1.1	20.33±0.03
24.097	TIRGO	<i>J</i>	4680	3.8	19.21±0.35
24.106	Loiano	<i>V</i>	2400	2.5	21.23±0.06
24.117	TIRGO	<i>K_s</i>	4680	3.3	17.49±0.25
24.127	Loiano	<i>R</i>	900	2.0	20.89±0.09
24.236	TNG	<i>R</i>	120	1.0	21.06±0.03
24.239	TNG	<i>R</i>	120	1.0	21.05±0.02
24.241	TNG	<i>I</i>	120	1.0	20.42±0.04
24.244	TNG	<i>I</i>	120	1.0	20.51±0.04
24.247	TNG	<i>V</i>	120	1.0	21.44±0.02
24.249	TNG	<i>V</i>	120	1.0	21.48±0.03
24.252	TNG	<i>B</i>	300	1.0	21.87±0.02
24.257	TNG	<i>B</i>	300	1.0	21.88±0.02
24.262	TNG	<i>U</i>	450	1.0	21.33±0.04
24.268	TNG	<i>U</i>	450	1.0	21.30±0.04
25.253	TNG	<i>R</i>	120	0.9	21.64±0.03
25.261	TNG	<i>V</i>	120	0.9	21.92±0.04
25.263	TNG	<i>V</i>	120	0.9	21.96±0.03
25.267	TNG	<i>B</i>	300	0.9	22.43±0.02
25.271	TNG	<i>B</i>	300	0.9	22.47±0.03
25.275	TNG	<i>I</i>	120	0.9	21.14±0.06
25.277	TNG	<i>I</i>	120	0.9	21.16±0.06
27.139	Asiago	<i>R</i>	900	3.1	22.11±0.25
27.264	TNG	<i>R</i>	360	1.2	22.38±0.05
27.270	TNG	<i>V</i>	360	1.1	22.80±0.06
27.278	TNG	<i>B</i>	360	1.1	23.28±0.08
Mar 31.226	TNG	<i>R</i>	3300	1.2	25.1±0.2

¹Magnitudes of the GRB counterpart, not corrected for interstellar absorption

²This measurement supersedes the value reported by Di Paola et al. (2001)

³This measurement supersedes the value reported by Bartolini et al. (2001)

second TNG *R*-band image. We chose standard Point Spread Function (PSF) fitting as photometric method, and to this aim we used the *DAOPHOT II* image data analysis package PSF-fitting algorithm (Stetson 1987) running within MIDAS¹. A two-dimensional Gaussian profile with two free parameters (the half width at half maxima along *x* and *y* coordinates of

each frame) was modeled on at least 5 unsaturated bright stars in each image. The errors associated with the measurements reported in Table 1 represent statistical uncertainties (at 1σ) obtained with the standard PSF-fitting procedure. In only one case, i.e. the TNG observation of Mar 31, we used aperture photometry for the magnitude determination as the PSF-fitting procedure could not give reliable results due to the faintness of the transient. In this case we used an aperture diameter equal to the seeing FWHM of the summed image.

¹ MIDAS (Munich Image Data Analysis System) is developed, distributed and maintained by ESO (European Southern Observatory) and is available at <http://www.eso.org/projects/esomidas>

Table 2. List of the absorption lines identified in the TNG optical spectrum of GRB010222 afterglow. The number associated with each line refers to the identification shown in Fig. 4. The error on all line positions can conservatively be assumed to be $\pm 3 \text{ \AA}$, i.e. comparable with the pixel size (see text). EWs of lines in the GRB rest frame, i.e. divided by a factor $(1+z)$, are also reported

Line number	Observed wavelength (\AA)	Rest frame wavelength (\AA)	Element	Redshift	W_{rest} (\AA)
1	3588	1862.790	AlIII	0.926 ± 0.002	2.1 ± 0.2
2	3979	2062.664	ZnII/CrII blend	0.929 ± 0.001	2.5 ± 0.3
3	4573	2374.461	FeII	0.926 ± 0.001	0.4 ± 0.2
4	4590	2382.765	FeII	0.926 ± 0.001	1.2 ± 0.3
5	5014	2600.173	FeII	0.928 ± 0.001	$0.7 \pm 0.3^*$
6	5384	2796.352	MgII	0.925 ± 0.001	0.7 ± 0.3
7	5401	2803.531	MgII	0.926 ± 0.001	1.1 ± 0.3
8	5500	2852.964	MgI	0.928 ± 0.001	0.6 ± 0.3
Weighted mean				0.927 ± 0.001	
9	3599	1670.787	AlII	1.154 ± 0.002	1.3 ± 0.4
10	3995	1854.716	AlIII	1.154 ± 0.002	0.8 ± 0.3
11	5060	2344.214	FeII	1.158 ± 0.001	0.7 ± 0.3
12	5133	2382.765	FeII	1.154 ± 0.001	0.6 ± 0.3
13	5573	2586.650	FeII	1.154 ± 0.001	1.1 ± 0.4
14	5603	2600.173	FeII	1.155 ± 0.001	1.0 ± 0.4
15	6024	2796.352	MgII	1.154 ± 0.001	0.7 ± 0.3
16	6038	2803.531	MgII	1.154 ± 0.001	1.2 ± 0.4
Weighted mean				1.155 ± 0.001	
17	3783	1526.707	SiII	1.478 ± 0.002	1.2 ± 0.3
18	3838	1550.774	CrV	1.475 ± 0.002	2.3 ± 0.2
19	4132	1670.787	AlII	1.473 ± 0.002	1.1 ± 0.3
20	4472	1808.013	SiII	1.474 ± 0.002	0.7 ± 0.3
21	5014	2026.136	ZnII/CrII blend	1.475 ± 0.001	$0.6 \pm 0.2^*$
22	5105	2062.664	ZnII/MgI blend	1.475 ± 0.001	1.1 ± 0.3
23	5800	2344.214	FeII	1.474 ± 0.001	2.2 ± 0.2
24	5880	2374.461	FeII	1.476 ± 0.001	1.9 ± 0.2
25	5894	2382.765	FeII	1.474 ± 0.001	1.7 ± 0.2
26	6384	2576.107	MnII	1.478 ± 0.001	0.5 ± 0.2
27	6401	2586.650	FeII	1.474 ± 0.001	0.8 ± 0.3
28	6423	2593.731	MnII	1.476 ± 0.001	2.0 ± 0.2
29	6435	2600.173	FeII	1.475 ± 0.001	1.9 ± 0.2
30	6454	2605.697	MnII	1.477 ± 0.001	1.1 ± 0.3
31	6919	2796.352	MgII	1.474 ± 0.001	2.8 ± 0.2
32	6937	2803.531	MgII	1.474 ± 0.001	3.4 ± 0.3
33	7069	2852.964	MgI	1.478 ± 0.001	1.0 ± 0.3
Weighted mean				1.475 ± 0.001	

*These lines might be blended with each other

To be consistent with magnitude measurements appeared on the GCN circulars archive², calibration was done using the *UBVRI* magnitudes, as measured by Henden (2001c), of field star ‘A’ indicated by Stanek et al. (2001a). However we used other field stars to check the stability of this calibration: we found it to be accurate to within 5%. Any significant short-term variation of star ‘A’ can be ruled out from our data. Due to the *U – B* color dependence of the DOLoReS CCD response in the *U* band, a ~ 0.2 mag color-term correction was subtracted from

the *U* magnitudes of the OT. We remark that the photometry errors quoted throughout the rest of the paper are only statistical and do not account for any possible (most likely very small) zero point offset.

We also retrieved and reduced the two *V*-band images obtained by Billings (2001) on 2001 Feb. 22.502 and 22.547 UT. From these, we obtain $V = 18.80 \pm 0.09$ and 19.11 ± 0.11 , respectively, assuming the calibration by Henden (2001c) as described above.

Standard procedures were used to reduce the NIR data: a sky estimate for each image was computed from the clipped

² GCN Circulars are available at: http://gcn.gsfc.nasa.gov/gcn/gcn3_archive.html

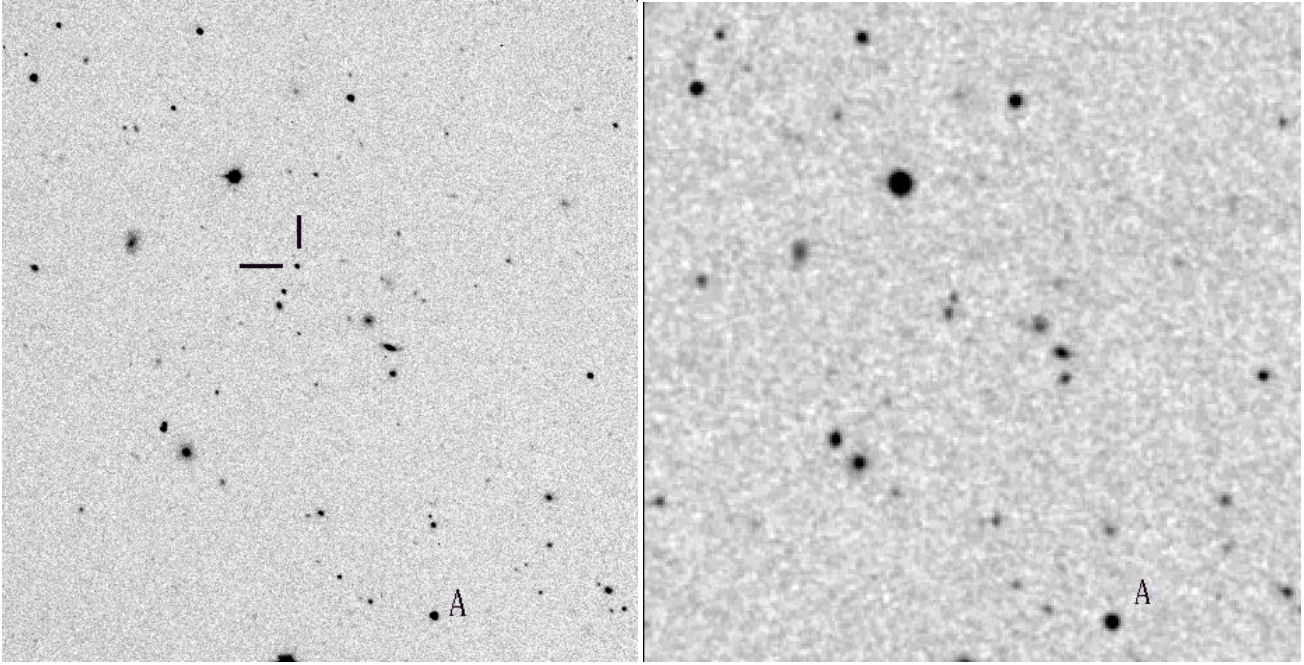


Fig. 1. (*Left panel*) Field of GRB010222 as imaged by the TNG on Feb 23.219 UT in the R band. The OT is indicated by the tickmarks. (*Right panel*) The same field as it appears on the DSS-II sky survey. No source is detected at the OT position. Both fields have a size of about $4' \times 4'$; North is at top and East is to the left. We also indicated the star ‘A’ by Stanek et al. (2001a), which we used for the calibration

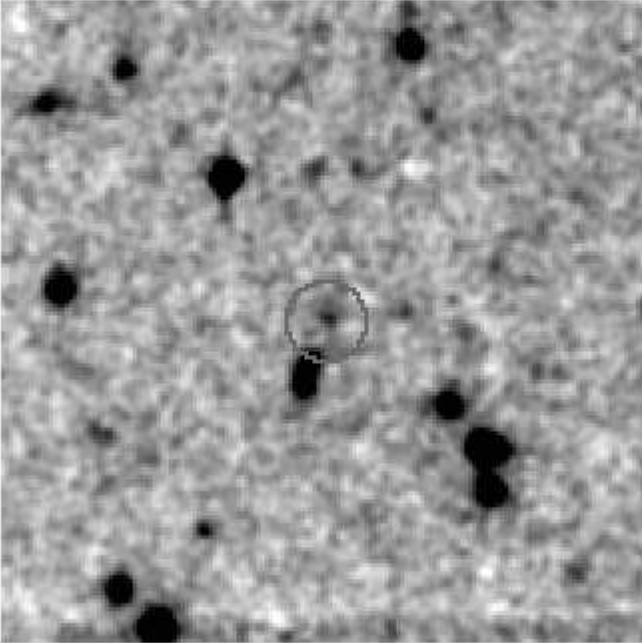


Fig. 2. Smoothed K_s -band image acquired at TIRGO on 2001 Feb 24.117 UT and centered at the NIR afterglow position. The image size is about $2.5' \times 2.5'$. North is at top, east is to the left. The circle indicating the position of the NIR transient has a radius of $15''$

median of the nearby images. The telescope dithering was measured from the offsets of field objects in each image and the images were averaged together using inter-pixel shifts. Magnitudes were measured inside circular apertures of diam-

eter $10''$ and corrected to total magnitudes. The photometric calibration was performed using NIR standard stars from the list by Hunt et al. (1998).

Given the poor seeing, the objects within $10''$ from the OT location could contribute to the measured NIR flux of the transient. It is not possible to accurately measure this effect, but we estimate that it is at most a small fraction of the total. Indeed, the peak of the emission is in good agreement with the expected position of the OT, and no evidence of flux is seen at the position of an object detected in the optical at about $5''$ north of the OT. Furthermore, the PSF profiles of the OT and of the object located $13''$ south-east of the OT itself are well distinguished, suggesting that the latter does not contaminate the OT flux (see Fig. 2).

We rescaled the TIRGO K_s magnitude to the standard K band. This was done in two steps: we first considered that, given the almost identical characteristics of the K_s and K' filters (Wainscoat & Cowie 1992) we could assume $K' = K_s$ within the large errors associated with our K_s measurement. Second, using the relation $K' - K = 0.2 \times (H - K)$ by Wainscoat & Cowie (1992) and assuming the power law spectral shape described in Section 3.3 to estimate the H -band magnitude of the OT, we obtained $K' - K \simeq 0.15$. Thus, $K = 17.35 \pm 0.3$ at the time of the TIRGO observation.

We then evaluated the Galactic absorption in the optical and NIR bands along the direction of GRB010222 using the Galactic dust infrared maps by Schlegel et al. (1998); from these data we obtained a color excess $E(B - V) = 0.022$. By applying the law by Rieke & Lebofsky (1985), this color excess corresponds to $A_V = 0.07$; then, using the relation by Cardelli

et al. (1989), we derived $A_U = 0.12$, $A_B = 0.09$, $A_R = 0.05$, $A_I = 0.04$, $A_J = 0.02$, $A_K = 0.01$.

Spectra, after correction for flat-field and bias, were background subtracted and optimally extracted (Horne 1986) using IRAF³. Helium-Argon lamps were used for wavelength calibration; spectra were then flux-calibrated by using the spectrophotometric standard Feige 34 (Massey et al. 1988) and finally averaged together. The correctness of the wavelength and flux calibrations was checked against the position of night sky lines and the photometric data collected around the epoch in which the spectra were acquired, respectively. The typical error was 0.5 Å for the wavelength calibration and 5% for the flux calibration.

3. Results

3.1. Photometry

We clearly detect the transient in all optical and NIR filters; Fig. 1 shows the TNG *R*-band image taken on 2001 Feb. 23.219 UT along with the same portion of sky as it appears on the DSS-II survey. The OT, indicated by the tickmarks, is clearly evident on the TNG image, while no object is present in the DSS-II image at that position. The association of this transient with GRB010222 is confirmed by the fading behaviour of this source (see optical magnitudes reported in Table 1). The light curves in *UBVRI* bands are reported in Fig. 3, where our data are complemented with those published by other authors (GCN circulars archive; Sagar et al. 2001; Stanek et al. 2001c; Cowsik & Bhargavi 2001). Note that we rescaled the *BVRI* magnitudes appeared in the GCN circulars to the zero point measured by Henden (2001c); we did not plot in Fig. 3 the measurements in GCN circulars which could not be tied to this photometric zero point (for instance, unfiltered or independently calibrated magnitudes). No correction has been applied for Galactic extinction, which is anyway small (see previous Section), to the data in Table 1 and Fig. 3; nor has any host galaxy continuum emission been subtracted, this being unknown at present.

We find that a single power law decay of the form $F \propto (t - t_0)^{-\alpha}$, where t_0 is the GRB start time, does not provide a satisfactory fit of the light curves. Indeed, considering a decay index $\alpha \sim 0.9$ as reported by Price et al. (2001b) and Fynbo et al. (2001b), we obtain a fit with $\chi_\nu^2 \sim 65$ over 68 degrees of freedom (dof). With this fit, the measurements acquired starting about 1 day after the GRB fall systematically below the expected decay. This is clearly evident in the *B*-, *V*- and *R*-band light curves, the best sampled since the first hours after the GRB.

We thus hypothesize that the *R*-band light curve can be modeled with a smoothly broken power law as the one used

by Stanek et al. (1999) to fit the optical light curves of the GRB990510 afterglow. The model we apply is:

$$F_\nu(t) = \frac{k_\nu}{\left(\frac{t}{t_b}\right)^{-\alpha_1} + \left(\frac{t}{t_b}\right)^{-\alpha_2}}, \quad (1)$$

where t_b is the time of the light curve break, α_1 is the asymptotic decay index for $t \ll t_b$ and α_2 is the asymptotic decay index for $t \gg t_b$ (times are expressed since t_0). Note that for the temporal decay indices we use inverted notations with respect to those of Stanek et al. (1999). We obtain a best fit of the *R*-band data with $\alpha_1 = 0.23 \pm 0.01$, $\alpha_2 = 1.57 \pm 0.01$ and $t_b = 0.54 \pm 0.01$ days after the GRB start time; however, this fit is not satisfactory, as it has $\chi_\nu^2 \sim 14$ (66 dof) and systematically underestimates the OT flux for $t > 5$ days after the GRB.

We next try the generalization adopted by Beuermann et al. (1999) of a smoothly broken power law model:

$$F_\nu(t) = (F_1(t)^{-s} + F_2(t)^{-s})^{-\frac{1}{s}}, \quad (2)$$

where $F_i(t) = k_i t^{-\alpha_i}$ (with $i = 1, 2$), and in which the parameter s indicates the smoothness of the change from a decay index to the other; for very large values of s , this function assumes a broken power law shape. This model fits much better ($\chi_\nu^2 = 1.6$, 65 dof) the *R* points than model of Eq. (1). An F-test shows that the model by Beuermann et al. (1999) leads to a tiny chance probability of improvement with respect to model of Eq. (1).

The formal fit parameters are: $\alpha_1 = 0.54 \pm 0.08$, $\alpha_2 = 1.31 \pm 0.02$, $t_b = 0.44 \pm 0.05$ days after the GRB start time, and ‘smoothness parameter’ $s = 3.1 \pm 1.0$. The value of this parameter indicates that the slope change occurred quite fastly around 12 hours after t_0 . However, the fit parameters α_1 and t_b are very sensitive to the value of s , and we have noted that similarly acceptable fits (χ_ν^2 ranging from 1.6 to 1.7) are obtained when s varies from ~ 3 to ~ 10 . Correspondingly, α_1 varies between ~ 0.5 and ~ 0.8 , and t_b between ~ 0.4 and ~ 0.7 days. The upper bounds of the intervals for these parameters are more consistent with the results of other authors (Sagar et al. 2001; Stanek et al. 2001c). Therefore, we will assume for α_1 and t_b their average values within the above ranges, and the associated dispersions as uncertainties: $\alpha_1 = 0.65 \pm 0.15$ and $t_b = 0.55 \pm 0.15$ days. The parameter α_2 is instead very weakly sensitive to the value of s .

The χ_ν^2 values associated with the fits are larger than 1 and therefore formally not completely satisfactory. By applying a systematic error of 1.5 % to all *R* data points, in addition to the statistical and calibration uncertainties, the χ_ν^2 becomes ~ 1 . Such a small additional uncertainty can be ascribed to non-homogeneity of *R*-band data set (acquired at different telescopes and analyzed using different methods), although small irregularities in the circumburst medium may produce in the afterglow light curve small time scale fluctuations of similar amplitude (e.g. GRB000301C, Masetti et al. 2000b; see also Wang & Loeb 2000).

The *U*, *B*, *V*, *I* and *J* light curves, albeit less well sampled, are consistent with the model describing the *R*-band data (see Fig. 3); therefore, no appreciable color evolution is present in the optical afterglow. On the contrary, the *K*-band light curve is consistent with being constant between the two epochs of observation.

³ IRAF is the Image Reduction and Analysis Facility made available at <http://iraf.noao.edu> to the astronomical community by the National Optical Astronomy Observatories, which are operated by AURA, Inc., under contract with the U.S. National Science Foundation. STSDAS is distributed by the Space Telescope Science Institute, which is operated by the Association of Universities for Research in Astronomy (AURA), Inc., under NASA contract NAS 5-26555.

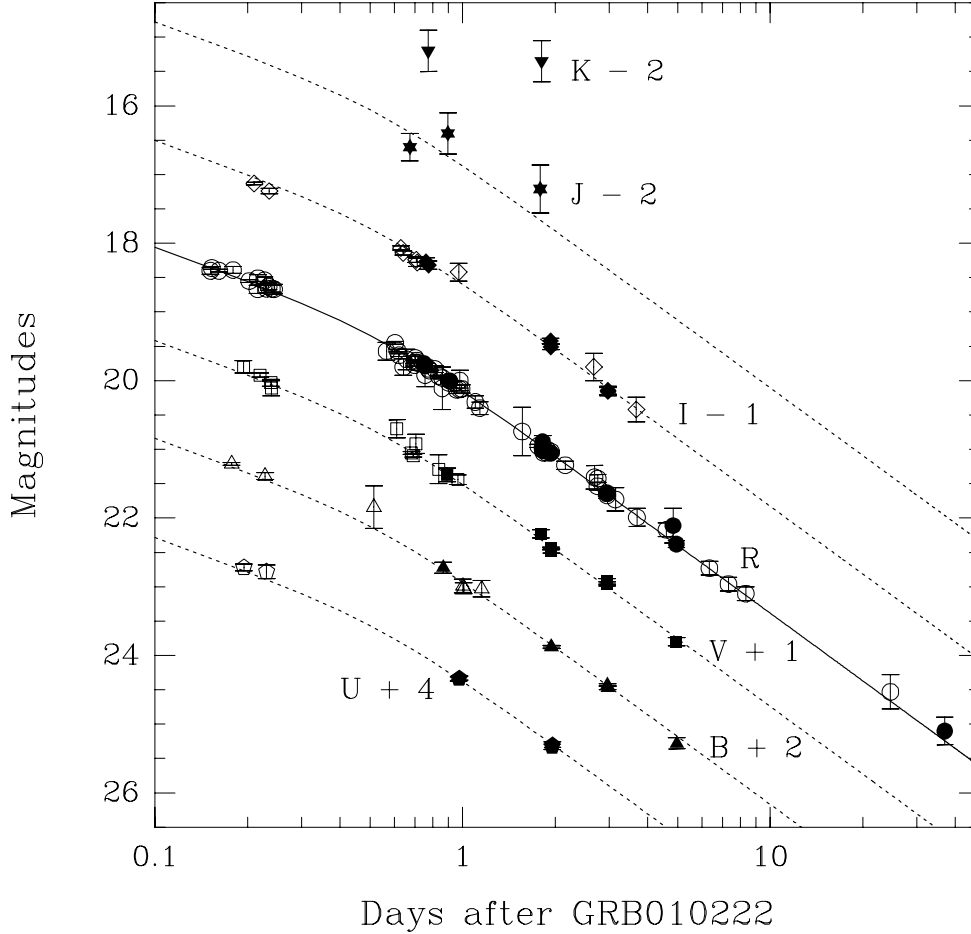


Fig. 3. *UBVR IJK* light curves of GRB010222 afterglow, based on the data presented in this paper and in the literature (see text). Different symbol styles indicate different bands. Filled symbols represent data presented in this work, while open symbols refer to measurements published by other authors. We have consistently referred all optical magnitudes to the calibration zero point of Henden (2001c). No Galactic extinction correction, nor host galaxy flux subtraction have been applied. The GRB start time corresponds to 2001 February 22.30799 UT. Overplotted to the *R*-band data (solid curve) is the best-fit double power law empirical model described in Sect. 3.1. Fit parameters are: $\alpha_1 = 0.65 \pm 0.15$, $\alpha_2 = 1.31 \pm 0.02$, $t_b = 0.55 \pm 0.15$ days. The same model curve, with unchanged model parameters, except for the flux normalization at the break time, accounts well for the data in the other bands (dashed curves), except *K*

From the fits, we obtained the following average color indices (not corrected for Galactic absorption): $U - B = -0.55 \pm 0.05$, $B - V = 0.43 \pm 0.05$, $V - R = 0.36 \pm 0.05$, $R - I = 0.55 \pm 0.05$ and $I - J = 0.72 \pm 0.15$. These figures place the OT of GRB010222 in the locus populated by GRB optical afterglows in the optical color-color diagrams, as illustrated by Šimon et al. (2001).

3.2. Spectroscopy

We detect several absorption features in the optical spectrum of the GRB010222 afterglow (Fig. 4). As earlier reported by other authors (Garnavich et al. 2001; Jha et al. 2001a,b; Bloom et al. 2001), these correspond to three different metal absorption systems located at different redshifts. Our line fitting, performed with the SPLIT task within IRAF, assumes a Gaussian profile

for the absorption lines. A conservative error of $\pm 3 \text{ \AA}$, comparable with the pixel size, is associated with each line wavelength measurement.

On the averaged TNG spectrum, presented in Fig. 4, we mark the positions of all lines we identified. Each number corresponds to a line in Table 2, where line wavelengths, identifications and redshifts are reported. From our line identifications we measure the three absorption systems at $z = 0.927 \pm 0.001$, $z = 1.155 \pm 0.001$ and $z = 1.475 \pm 0.001$, the highest one thus being the lower limit for the redshift of this GRB. These results are consistent with those of Garnavich et al. (2001), Jha et al. (2001a,b) and Bloom et al. (2001). Our spectral resolution is not sufficient to confirm the presence of a fine structure in the farthest absorbing system as reported by Castro et al. (2001).

In Table 2 we also list the equivalent widths (EWs) of the identified lines computed in the absorber rest frame (i.e. by di-

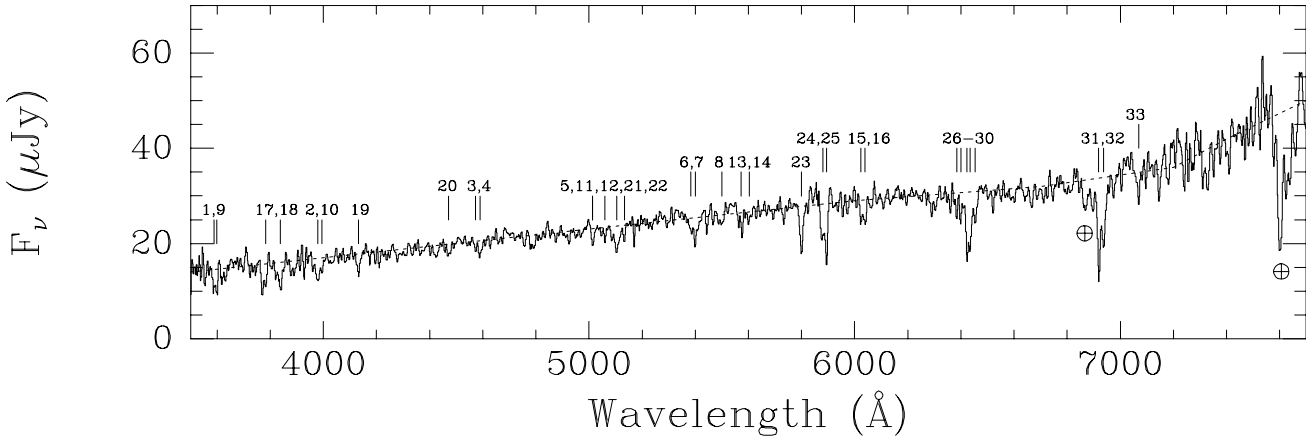


Fig. 4. TNG+DOLoReS spectrum of the GRB010222 afterglow in the 3500-7700 Å range, smoothed with a Gaussian filter with $\sigma=3$ Å (i.e. comparable with the spectral dispersion) and corrected for Galactic absorption assuming $E(B-V) = 0.022$. Numbers mark the positions of identified lines as listed in Table 2. Telluric absorption lines at 6870 and 7600 Å are also marked with the symbol \oplus . The dashed curve indicates the position of the spectral continuum we used to measure the EW of lines

viding the measured value by the factor $1+z$). The errors on the EWs are computed by assuming different spectral continuum levels roughly corresponding to 1σ variation of the continuum itself in proximity of each line.

It can be noted from Table 2 that the metal lines of the absorption system at the highest z are very strong. In particular, the detection of MgI suggests that the optical emission of the GRB afterglow pierced through a dense medium, most likely that of a host galaxy at $z=1.475$. If we consider the study of $z < 1.65$ MgII systems in QSO spectra by Rao & Turnshek (2000) we find that, according to these authors, MgII systems with rest frame EW of $\text{MgII}\lambda 2796 \geq 0.6$ Å are primarily associated with Damped Lyman- α Absorption (DLA) systems. DLAs are characterized by being mostly HI interstellar medium clouds of high redshift galaxies. Indeed, about 50% of the Rao & Turnshek’s (2000) sample of MgII absorbers with $\text{MgII}\lambda 2796$ and $\text{FeII}\lambda 2600$ EWs larger than 0.5 Å have HI column density $N_{\text{HI}} > 2 \times 10^{20}$ atoms cm^{-2} and basically all have $N_{\text{HI}} > 10^{19}$ atoms cm^{-2} .

Moreover, they found that almost all DLAs with $N_{\text{HI}} > 2 \times 10^{20}$ atoms cm^{-2} have $\text{MgI}\lambda 2852$ EW larger than 0.7 Å. Thus, given the EWs of MgI, FeII and MgII reported in Table 2, we have good indications that the $z=1.475$ absorber, if not associated with the GRB itself, most likely resembles the properties of a DLA system with column density $N_{\text{HI}} > 2 \times 10^{20}$ atoms cm^{-2} . The ratio of the EWs of the MgII doublet is $W_{\text{rest}}(\lambda 2796)/W_{\text{rest}}(\lambda 2803) = 0.8 \pm 0.1$; this indicates that the absorption is saturated and, given the low resolution of the spectrum, the column density is undetermined. Rao & Turnshek (2000) also show that there is no precise relationship between the HI column density and the rest frame EW of $\text{MgII}\lambda 2796$. Thus, although we have good indications that the $z=1.475$ system bears substantial absorption, the HI column density is basically unknown. Applying the same approach to the other two absorption systems lying along the GRB line of

sight (although in the case of the absorber at $z=1.155$ no MgI is detected), we suggest that these systems have a HI column density in excess of 10^{19} atoms cm^{-2} . All this points to the possibility of the presence of additional extragalactic absorption along the GRB010222 line of sight.

Finally, we tested the hypothesis (Sari et al. 1998) that the optical spectrum can be described with a power law in the form $F_\nu \propto \nu^{-\beta}$. If we fit the TNG spectrum with this law, we obtain $\beta = 1.16 \pm 0.05$ (with $\chi_\nu^2 \sim 1$), consistent with the fit results from the multiwavelength spectra shown in the next Subsection, but somewhat steeper than the value reported by Jha et al. (2001b).

3.3. Multiwavelength spectra

In order to study the temporal evolution of the multiwavelength spectrum of the GRB010222 afterglow, we have selected 5 epochs from ~ 0.2 to ~ 5 days after the high-energy event, at which best spectral sampling is available. We corrected the afterglow optical/NIR magnitudes for the Galactic absorption and converted them into fluxes using the tables by Fukugita et al. (1995) for the optical and by Bersanelli et al. (1991) for the NIR. If strictly simultaneous observations are not available, we reduced the fluxes to the reference epoch by interpolating the empirical model fitted to the R -band light curve (see Sect. 3.1), and normalizing to the appropriate band. A 7% systematic error is added quadratically to the measurements to account for interpolation and magnitude-to-flux conversion uncertainties. The results are plotted in Fig. 5.

The optical spectral distributions covering B , V , R and, when available, U and I filters are well fit at all epochs by a single power law of average spectral index $\beta = 1.1 \pm 0.1$ (the χ_ν^2 is typically ~ 1). A constant spectral shape is consistent with the achromatic evolution of the OT decay.

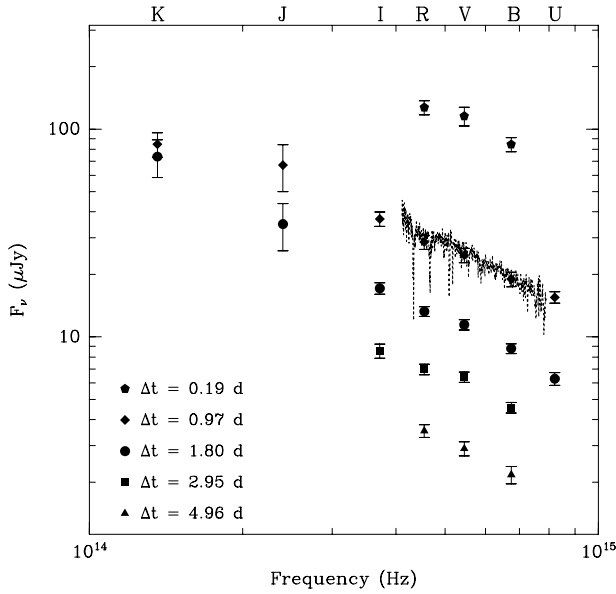


Fig. 5. Optical/NIR broad-band spectra of the GRB010222 afterglow at five different epochs: 0.19, 0.97, 1.80, 2.95, and 4.96 days after the GRB. The data are corrected for Galactic absorption. A 7% systematic error was added quadratically to the measurement errors in order to account for interpolation and magnitude-to-flux conversion uncertainties. For the sake of comparison, we also plotted the TNG optical spectrum reported in Fig. 4 (acquired at epoch $\Delta t = 1.04$ days after the GRB)

A single power law fit to the *UBVRIJK* data at the third epoch gives $\beta = 1.3 \pm 0.1$ with $\chi^2_\nu = 2.3$ (5 dof), slightly steeper than the optical slope. Although this may suggest some absorption within the host galaxy in addition to the Galactic one (e.g., Lee et al. 2001), we note that the difference is barely significant, considering the uncertainty on the joint optical/NIR spectral fit. Therefore we conclude that the optical spectra at all epochs and the optical/NIR spectrum at 1.8 days after the GRB do not deviate significantly from a single power law of slope $\beta \simeq 1$.

On the contrary, the *K*-band point at the second epoch ($\Delta t = 0.97$ days after the GRB) strongly deviates from this trend. If we attempt to fit all *UBVRIJK* points at this epoch with a single power law we obtain an unacceptable fit.

4. Discussion

The optical light curves of the GRB010222 afterglow are described by a continuously steepening trend, instead of a single power law, a behaviour seen in about 1/3 of the well monitored optical afterglows (GRB980519, Jaunsen et al. 2001; GRB990123, Castro-Tirado et al. 1999; GRB990510, Stanek et al. 1999; GRB990705, Masetti et al. 2000a; GRB991208, Castro-Tirado et al. 2001; GRB991216, Halpern et al. 2000; GRB000301C, Masetti et al. 2000b, Jensen et al. 2001; GRB000926, Fynbo et al. 2001a). In the present case, this can-

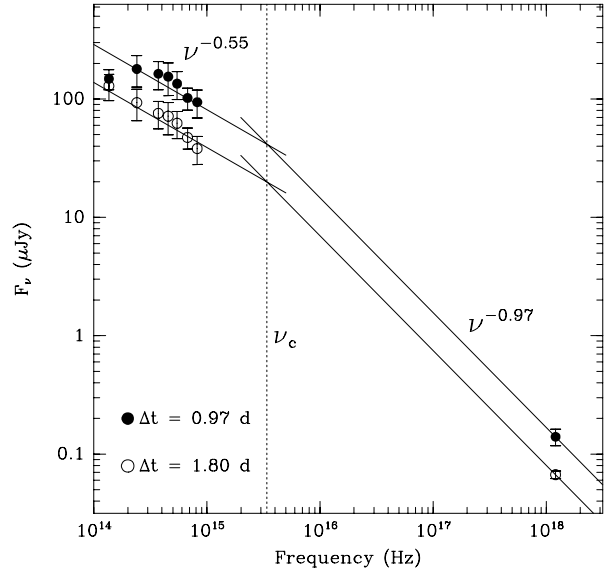


Fig. 6. Multiwavelength X-ray/optical/NIR SEDs of the GRB010222 afterglow at epochs 0.97 and 1.8 days after the GRB. The X-ray data are from in 't Zand et al. (2001). Optical and NIR data were corrected both for Galactic extinction and for intrinsic host galaxy absorption using the extinction curve by Calzetti (1997) and a local color excess $E(B - V) = 0.35$. The resulting optical/NIR spectrum has a slope $\beta \sim 0.55$ at both epochs (the *K*-band point of the first epoch was excluded from the fit because highly deviant). This plot indicates that ν_c lies between the optical and X-ray ranges, at $\simeq 3.5 \times 10^{15}$ Hz

not be ascribed to the synchrotron cooling frequency ν_c crossing the optical band in a spherical regime (Sari et al. 1998), because the expected variation of decay index would be in this case much smaller ($\Delta\alpha = 0.25$) than observed ($\Delta\alpha \simeq 0.75$). Moreover, although the limited optical band hampers a neat distinction, the ν_c transition should be wavelength dependent, while the observed steepening is achromatic.

Therefore we have considered a decelerating and sideways expanding jet scenario (Sari et al. 1999). In this case, the index α_2 should equal the index of the electron energy distribution, thus $p = 1.3$. From this follows that the optical decay index before the collimation break time must be $\alpha_1 = 0.23$, in case ν_c is above the optical band at those epochs. This is rather different from our value of α_1 , 0.65 ± 0.15 . Therefore, within the present picture, at the observing epochs preceding the collimation break time, ν_c should have already crossed the optical band, so that the predicted α_1 would be ~ 0.5 , more similar to its observed value. The slope of the optical spectrum should then be $p/2 \simeq 0.7$, significantly flatter than both our measured value $\beta = 1.1$ and that ($\beta = 0.9$) reported by Jha et al. (2001b).

Local absorption, on top of the Galactic extinction, may account for the difference (see below), but would lead to an intrinsic optical spectral slope rather different than found in X-rays ($\beta_X \simeq 1$; in 't Zand et al. 2001), which is inconsistent with

the fact that both bands should be above ν_c . In addition, the index of the electron energy distribution derived in the sideways expanding jet scenario, $p = 1.3$, is very flat (in general, p values larger than 2 are found; see Frontera et al. 2000) and may pose energetic problems (although one can assume that the electron power law has a cut-off at some energy). Emission from the still undetected host galaxy of GRB010222 may flatten the late epoch light curve of the afterglow, but the most recent R -band photometry (our Fig. 3; Stanek et al. 2001c; Sagar et al. 2001) suggests that the total magnitude of the host cannot be brighter than $R \simeq 27$ and that its contribution at the latest monitoring epochs (~ 40 days after the GRB) is not significant, so that subtracting it from the optical measurements does not alter the fitted value of α_2 , and therefore of p .

Given the problems posed by the application of the above model to our optical/NIR afterglow data, we have considered two alternatives.

First we have compared our results with a model of an external shock expanding in a pre-ejected wind, which determines a r^{-2} dependence for the medium density (Panaitescu & Kumar 2000). In the optical/NIR bands, it is predicted that, at the early epochs (up to 0.1 days after explosion in the source rest frame), the temporal decay is significantly flatter ($\alpha_1 = 0.25$) than found by us, while at later epochs our measured α_2 can be reproduced with $p = 2.1$, which is acceptable.

Then, we have made the hypothesis that the temporal break observed in the optical light curves may be generated by the transition from relativistic to non-relativistic conditions in the shock (Dai & Lu 1999). By applying the prescriptions of Dai & Lu (1999) to our measured decay indices we obtain compatible conditions on p only if the ν_c is above the optical band during our monitoring. From $\alpha_1 = 0.65 \pm 0.15$ and $\alpha_2 = 1.31 \pm 0.02$ we derive $p = 1.9 \pm 0.2$ and $p = 2.27 \pm 0.01$, respectively, which we consider marginally consistent with $p \sim 2.1$ - 2.2 . This appears to be an acceptable value for the electron distribution shape. The predicted spectrum, for $\nu_{\text{opt}} < \nu_c$, is $\beta \simeq 0.6$, much flatter than observed. We have made the hypothesis that intrinsic absorption at the source produces the observed steeper spectrum and we have searched for a de-extinction curve to correct for this.

As noted by Jha et al. (2001b), the optical spectrum lacks, at rest frame $z = 1.475$, the typical 2175 Å dust absorption wide feature seen in the reddening curve of the Milky Way (Pei 1992, Cardelli et al. 1989) and of star forming galaxies (e.g. Calzetti 1997). Thus, intrinsic absorption must not be large. We have considered both an extinction curve appropriate for starburst galaxies (Calzetti 1997) and the SMC curve (Pei 1992), and applied them to our data. With the latter curve we cannot reproduce the predicted spectral slope in the optical/NIR wavelength range for any value of $E(B - V)$ (while in the optical range only, acceptable fits are obtained, see also Lee et al. 2001). The starburst curve provides instead an acceptable correction and reproduces power-law spectra (except for the deviating K -band point at epoch 0.97 days) with index $\beta \sim 0.5$ for a moderate color excess, $E(B - V) \sim 0.35$ (see Fig. 6). The corrected optical/NIR spectral index is much flatter than that found in X-rays, which suggests that ν_c lies between the optical and X-

ray bands. This is strengthened by the consistency of the X-ray spectral index with $p/2$.

An empirical value of $\nu_c \simeq 3.5 \times 10^{15}$ Hz (supposed to be nearly constant during the non-relativistic expansion, Dai & Lu 1999) is determined through the extrapolation of the optical and X-ray spectra (Fig. 6). The hypothesis of extinction within a heavily star forming host galaxy has the advantage of removing the mismatch between the optical and X-ray spectra normalizations (otherwise attributable to other causes, like inverse Compton emission in the X-rays, as suggested by in 't Zand et al. 2001), and had been applied in a similar context also to GRB971214 (Dal Fiume et al. 2000).

The J -band light curve behaviour is similar to that of the optical ones, indicating that the injection break frequency ν_m is below this band at both epochs of NIR observations. However, the behaviour of the K -band light curve deviates significantly from that observed at shorter wavelengths. Comparison of the broad-band spectra at 0.97 and 1.8 days after GRB could suggest that the injection break may be located between the K and J bands at the former epoch, and has moved below the K band at the latter. Although this would be consistent with the evolution time scale of $\nu_m (\propto t^{-3/2})$, the higher fluxes detected at sub-mm wavelengths at preceding and successive epochs, indicate that the injection break should be located longward of the NIR band during our monitoring (Fich et al. 2001; Kulkarni et al. 2001). Therefore, we have no straightforward explanation for the deviation of the K -band point from a single optical-to-NIR power-law at 0.97 days.

At $z = 1.475$, the total isotropic energy emitted in the 2-700 keV range by this GRB is 7.7×10^{53} erg (in 't Zand et al. 2001). With this total energy, and assuming a circumburst medium density of $n = 10^5 - 10^6 \text{ cm}^{-3}$, the epoch of the transition from ultrarelativistic to non-relativistic conditions is about 1 day (Dai & Lu 1999). Therefore, the most viable interpretation of our data appears to be a shock undergoing a substantial deceleration and transition to non-relativistic conditions at about 0.5 days after the GRB (see also Dai & Cheng 2001). The consequent requirement of a thick ambient medium (denser than 10^6 cm^{-3}) is supported by the observation of the absorbing system at $z = 1.475$, likely coinciding with the redshift of the source. This density would be typical for starburst galaxies (Calzetti 1997) or DLAs (Wolfe et al. 1986; Rao & Turnshek 2000), and is similar to that found for a number of GRB hosts (GRB990510, Vreeswijk et al. 2001; GRB000301C, Jensen et al. 2001; GRB000926, Fynbo et al. 2001a). Therefore, as for many previous OTs, there is the suggestion that GRB010222 occurred in a site of substantial star formation.

Our observations and conclusions point to the importance of early optical/NIR monitoring of GRB afterglows to establish their behaviour and to get insight into the GRB progenitor. This will be guaranteed by the current (HETE-2) or soon-to-fly GRB missions (*AGILE* and *Swift*).

Acknowledgements. We thank the staff astronomers of the TNG, Asiago, Loiano, Campo Imperatore and TIRGO Observatories. We also thank the anonymous referee for comments and suggestions which helped us improving the paper. We acknowledge Scott Barthelmy for maintaining the GRB Coordinates Network (GCN) and

BACODINE services; the *BeppoSAX* e-mail GRB Alert Service is also acknowledged. Krzysztof Stanek is thanked for having noted a discrepancy between our *U*-band calibration and his, and for exchanging his *U*-band data with us. C. Bartolini, A. Guarnieri, and A. Piccioni acknowledge the University of Bologna (Funds for Selected Research Topics).

References

- Bartolini, C., Bernabei, S., Guarnieri, A., et al., 2001, GCN 982
 Berger, E., & Frail, D.A., 2001, GCN 968
 Bersanelli, M., Bouchet, P., & Falomo, R., 1991, A&A, 252, 854
 Beuermann, K., Hessman, F.V., Reinsch, K., et al., 1999, A&A, 352, L26
 Billings, G., 2001, GCN 969
 Bloom, J.S., Djorgovski, S.G., Halpern, J.P., et al., 2001, GCN 989
 Calzetti, D., 1997, AJ, 113, 162
 Cardelli, J.A., Clayton, G.C., & Mathis J.S., 1989, ApJ, 345, 245
 Castro, S., Djorgovski, S.G., Kulkarni, S.R., et al., 2001, GCN 999
 Castro-Tirado, A.J., Gorosabel, J., Zapatero-Osorio, M.R., et al., 1999, Science, 283, 2069
 Castro-Tirado, A.J., Sokolov, V.V., Gorosabel, J., et al., 2001, A&A, 370, 398
 Chevalier, R.A., & Li, Z.Y., 1999, ApJ, 520, L59
 Chevalier, R.A., & Li, Z.Y., 2000, ApJ, 536, 195
 Cowsik, R., & Bhargavi, S.G., 2001, GCN 1051
 Dai, Z.G., & Lu, T., 1999, ApJ, 519, L155
 Dai, Z.G., & Cheng, K.S., 2001, ApJ, submitted (astro-ph/0105055)
 Dal Fiume, D., Amati, L., Antonelli, L.A., et al., 2000, A&A, 355, 454
 Di Paola, A., Antonelli, L.A., Li Causi, G., & Valentini, G., 2001, GCN 977
 Fich, M., Phillips, R.M., Tilanus, R.P.J., Frail, D.A., & Smith, I., 2001, GCN 971
 Frontera, F., Amati, L., Costa, E., et al., 2000, ApJS, 127, 59
 Fruchter, A.S., Thorsett, S.E., Metzger, M.R., et al. 1999, ApJ, 519, L13
 Fukugita, M., Shimasaku, K., & Ichikawa, T., 1995, PASP, 107, 945
 Fynbo, J.P.U., Gorosabel, J., Dall, T.H., et al., 2001a, A&A, in press (astro-ph/0102158)
 Fynbo, J.P.U., Gorosabel, J., Jensen, B.L., et al., 2001b, GCN 975
 Gandolfi, G., 2001, GCN 966
 Garnavich, P.M., Pahre, M.A., Jha, S., et al., 2001, GCN 965
 Halpern, J.P., Uglesich, R., Mirabal, N., et al., 2000, ApJ, 543, 697
 Harrison, F.A., Bloom, J.S., Frail, D.A., et al., 1999, ApJ, 523, L121
 Henden, A., 2001a, GCN 961
 Henden, A., 2001b, GCN 962
 Henden, A., 2001c, GCN 987
 Henden, A., & Vrba F., 2001, GCN 967
 Horne, K., 1986, PASP, 98, 609
 Hunt, L.K., Mannucci, F., Testi, L., et al., 1998, AJ, 115, 2594
 in 't Zand, J.J.M., Kuiper, L., Amati, L., et al., 2001, ApJ, submitted, astro-ph/0104362
 Israel, G.L., Marconi, G., Covino, S., et al., 1999, A&A, 348, L5
 Jaunsen, A.O., Hjorth, J., Björnsson, G., et al., 2001, ApJ, 546, 127
 Jensen, B.L., Fynbo, J.P.U., Gorosabel, J., et al., 2001, A&A, 370, 909
 Jha, S., Matheson, T., Calkins, M., et al., 2001a, GCN 974
 Jha, S., Pahre, M.A., Garnavich, P.M., et al., 2001b, ApJ, in press, (astro-ph/0103081)
 Klose, S., Stecklum, B., Masetti, N., et al., 2000, ApJ, 545, 271
 Kulkarni, S.R., Djorgovski, S.G., Odewahn S.C., et al., 1999, Nat, 398, 389
 Kulkarni, S.R., Frail, D.A., Moriarty-Schieven, G., et al., 2001, GCN 996
 Lee, B.C., Tucker, D.L., Vanden Berk, D.E., et al., 2001, ApJ, submitted (astro-ph/0104201)
 Masetti, N., Palazzi, E., Pian E., et al., 2000a, A&A, 354, 473
 Masetti, N., Bartolini, C., Bernabei, S., et al., 2000b, A&A 359, L23
 Masetti, N., Palazzi, E., Pian, E., et al., 2001, GCN 985
 Massey, P., Strobel, K., Barnes, J.V., & Anderson, E., 1988, ApJ, 328, 315
 McDowell, J., Kilgard, R., Garnavich, P.M., Stanek, K.Z., & Jha, S., 2001, GCN 963
 Palazzi, E., Pian, E., Masetti N., et al., 1998, A&A, 336, L95
 Panaitescu, A., & Kumar, P., 2000, ApJ, 543, 66
 Pei, W., 1992, ApJ, 395, 130
 Piro, L., 2001a, GCN 959
 Piro, L., 2001b, GCN 960
 Price, P.A., Harrison, F.A., Galama, T.J., et al., 2001a, ApJ, 549, L7
 Price, P.A., Gal-Yam, A., Ofek, E., et al., 2001b, GCN 973
 Rao, S.M., & Turnshek, D.A., 2000, ApJS, 130, 1
 Rhoads, J.E., 1999, ApJ, 525, 737
 Rieke, G.H., & Lebofsky, M.J., 1985, ApJ, 288, 618
 Sagar, R., Stalin, C.S., Bhattacharya, D., et al., 2001, Bull. Astron. Soc. India, submitted (astro-ph/0104249)
 Sari, R., Piran, T., & Narayan, R., 1998, ApJ, 497, L17
 Sari, R., Piran, T., & Halpern, J.P., 1999, ApJ, 519, L17
 Schlegel, D.J., Finkbeiner, D.P., & Davis, M., 1998, ApJ, 500, 525
 Šimon, V., Hudec, R., Pizzichini, G., & Masetti, N., 2001, A&A, submitted
 Stanek, K.Z., Garnavich, P.M., Kaluzny, J., et al., 1999, ApJ, 522, L39
 Stanek, K.Z., Jha, S., McDowell, J., et al., 2001a, GCN 970
 Stanek, K.Z., Garnavich, P., Jha, S., & Pahre, M., 2001b, IAU Circ. 7586
 Stanek, K.Z., Garnavich, P.M., Jha S., et al., 2001c, ApJ, submitted (astro-ph/0104329)
 Stetson, P.B., 1987, PASP, 99, 191
 Vreeswijk, P.M., Fruchter, A.S., Kaper, L., et al., 2001, ApJ, 546, 672
 Wainscoat, R.J., & Cowie, L.L., 1992, AJ, 103, 332
 Wang, X., & Loeb, A., 2000, ApJ, 535, 788
 Wolfe, A.M., Turnshek, D.A., Smith, H.E., & Cohen, R.D., 1986, ApJS, 61, 249